Report

Maternal Origins of Developmental Reproducibility

Mariela D. Petkova,[1] Shawn C. Little,[2] Feng Liu,[1] and Thomas Gregor[1,3,*]

[1]Joseph Henry Laboratories of Physics, Princeton University, Princeton, NJ 08544, USA
[2]Department of Molecular Biology, Howard Hughes Medical Institute, Princeton University, Princeton, NJ 08544, USA
[3]Lewis-Sigler Institute for Integrative Genomics, Princeton University, Princeton, NJ 08544, USA

Summary

Cell fate decisions during multicellular development are precisely coordinated, leading to highly reproducible macroscopic structural outcomes [1–3]. The origins of this reproducibility are found at the molecular level during the earliest stages of development when patterns of morphogen molecules emerge reproducibly [4, 5]. However, although the initial conditions for these early stages are determined by the female during oogenesis, it is unknown whether reproducibility is perpetuated from oogenesis or reacquired by the zygote. To address this issue in the early *Drosophila* embryo, we sought to count individual maternally deposited *bicoid* mRNA molecules and compare variability between embryos with previously observed fluctuations in the Bicoid protein gradient [6, 7]. Here, we develop independent methods to quantify total amounts of mRNA in individual embryos and show that mRNA counts are highly reproducible between embryos to within ∼9%, matching the reproducibility of the protein gradient. Reproducibility emerges from perfectly linear feedforward processes: changing the genetic dosage in the female leads to proportional changes in both mRNA and protein numbers in the embryo. Our results indicate that the reproducibility of the morphological structures of embryos originates during oogenesis, which is when the expression of maternally provided patterning factors is precisely controlled.

Results

Cells along the anterior-posterior (AP) axis of the developing *Drosophila* embryo determine their location by interpreting concentrations of morphogen molecules that correlate with AP position. One process leading to these molecular patterns (reviewed in [8]) originates in the female during oogenesis when maternal mRNA of the anterior determinant *bicoid* (*bcd*) is localized at the anterior pole of the egg. Upon egg activation, these mRNA molecules serve as sources for a protein gradient, which triggers a network of interacting genes that generate a cascade of increasingly diversified molecular spatial patterns, eventually specifying unique fates for each of the ∼80 rows of cells along the AP axis [9]. The diffusion-driven, exponentially decaying concentration profile of Bcd protein is reproducible to within 10% from embryo to embryo [7], which is sufficient to encode position with 1.6% embryo

length (EL) precision. Spatial precision is observed in all features of the subsequent molecular and morphologic patterns [10–13], including the first macroscopic structure in the embryo, the cephalic furrow [14–16]. It is unknown, however, whether such high reproducibility is also realized at the level of maternal mRNA. Is reproducibility of the protein gradient determined during oogenesis, or is it acquired in the embryo via specialized error-correcting mechanisms [5, 12, 17]? Here, we test whether the expression of *bcd* during oogenesis is controlled with 10% or better precision and determine the quantitative, mechanistic constraints on the amount of mRNA deposited into the oocyte.

To address whether the female confers reproducibility to the zygote through control of mRNA, we devised two strategies to quantify *bcd* mRNA molecules in individual embryos. Measuring reproducibility in intact embryos requires a measurement error that is low compared to the actual embryo-to-embryo fluctuations in mRNA numbers; we therefore sought to count individual molecules, which can only be achieved by an optical method. In wild-type embryos, optically resolving individual *bcd* mRNA molecules is hindered by the packaging of *bcd* mRNA into ribonuclear protein complexes containing variable multiples of mRNAs [18]. The formation of these particles requires the protein Staufen (Stau) [19]. Therefore, we optically measured *bcd* mRNA in embryos from *stau* mutant females (referred to hereafter as *stau*⁻ embryos) and developed an alternative counting method based on bulk quantitative PCR (qPCR) measurements to confirm that our results also apply to wild-type.

Total mRNA Counts in Individual Intact Embryos

To optically identify individual mRNA molecules in whole-mount embryos and to assess embryo-to-embryo reproducibility, we extended a recently developed mRNA labeling method of fluorescence in situ hybridization (FISH) [18, 20]. We labeled *bcd* mRNAs with synthetic probes and then counted individual molecules and measured their fluorescence intensity by confocal microscopy (Figure 1; Figure S1 available online). In wild-type embryos, this technique revealed a bimodal intensity distribution of *bcd* mRNA particles (Figures 1A and S1B) held together by Stau [19]. We resolved these *bcd* complexes into individual mRNA molecules in *stau*⁻ embryos (Figure 1B) [20], with a unimodal particle intensity distribution (Figure S1B). We counted M_{bcd}^{FISH} = (8.9 ± 0.3) × 10^5 *bcd* mRNA molecules in individual *stau*⁻ embryos; the error bar is the SE of the mean across n = 7 embryos (Supplemental Experimental Procedures).

To confirm that the number of *bcd* mRNA molecules in *stau*⁻ embryos was comparable to that of wild-type, we modified a widely used PCR technique [21] to count molecules in wild-type and *stau*⁻ embryos. This technique also allowed us to verify that the fluorescent particles in *stau*⁻ embryos corresponded to individual mRNA molecules. In quantitative RT-PCR (qRT-PCR), mRNA molecules are chemically extracted from the sample, converted to DNA by reverse transcription, and subsequently quantified by real-time PCR amplification using a SYBR Green fluorescence reporter. Usually, qRT-PCR cannot measure absolute mRNA in biological samples, mainly due to challenges in quantifying the process of
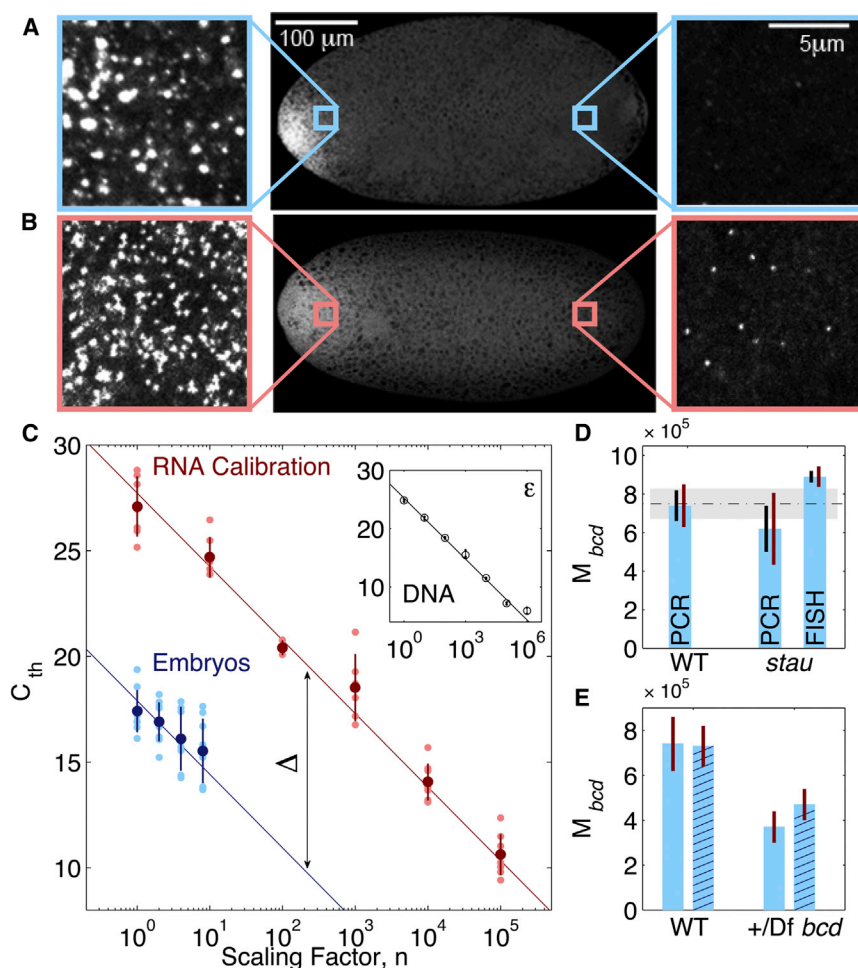
*Correspondence: tg2@princeton.edu

Figure 1. Two Independent Methods Measure ~750,000 *bcd* mRNA Molecules in Individual Embryos

(A and B) In situ total mRNA measurements using single-molecule counting. *bcd* mRNA molecules in fixed embryos are tagged with 90 fluorescently labeled oligonucleotide probes (20-mer) for wild-type (A) and *stau⁻* mutant (B) embryos. Particles containing multiple *bcd* mRNA molecules dissociate in *stau⁻* mutants (side panels), as apparent from unimodal particle intensity distribution (Figure S1).

(C) Bulk mRNA is extracted from individual samples (colored data points), converted to cDNA, and quantified via qPCR. Threshold cycle C_{th} refers to the PCR amplification cycle for which the sample fluorescence reaches an arbitrary predefined threshold at which all samples are compared. DNA dilution series (inset) measures the PCR amplification efficiency $\varepsilon = 10^{-1/\text{slope}}$ ($\varepsilon = 1.98$; error bars are smaller than data markers). An RNA calibration (red) is constructed from samples with $n \times M_{\text{ref}}$ synthetically generated mRNA molecules. An embryo series (blue) is constructed from samples containing n = (1, 2, 4, 8) embryos (10–30 min old). The slope of the blue and red lines is set by ε, and the offset (Δ) between the lines determines the number (M_{bcd}) of total mRNA molecules per embryo (Supplemental Experimental Procedures).

(D) qRT-PCR measurements of total *bcd* mRNA in wild-type and *stau⁻* embryos yield a mean of $7.4 \times 10^5 \pm (0.8, 1.1) \times 10^5$ (SEM, measurement error) and $6.2 \times 10^5 \pm (1.2, 1.9) \times 10^5$ molecules, respectively. SEM is shown as black bars. Measurement errors are estimated from the single-parameter fitting (red bars). With FISH in seven *stau⁻* embryos, $(8.9 \pm 0.3) \times 10^5$ molecules are detected (error is SEM; we estimate the overall FISH measurement error to be ~6%). Dashed horizontal line and gray shading correspond to the mean of the three measurements and the SEM, i.e., $M_{bcd} = (7.5 \pm 0.8) \times 10^5$.

(E) qRT-PCR measurements of total *bcd* mRNA counts from two independent large-scale experiments (empty and hashed bars) are $(7.4 \pm 1.2) \times 10^5$ and $(7.3 \pm 0.9) \times 10^5$ in wild-type embryos (two *bcd* DNA copies) and $(4.7 \pm 0.7) \times 10^5$ and $(3.7 \pm 0.7) \times 10^5$ in +/Df *bcd* embryos (one *bcd* DNA copy). The number of samples in each experiment is found in Table S1.

mRNA isolation [22, 23]. By quantifying all systematic errors along the different processing steps, we developed a scheme to accurately estimate *bcd* mRNA molecules in individual embryos.

In our strategy, the largest quantitative effect was achieved through controlling for losses associated with RNA isolation; mRNA molecules from homogenized embryos were compared to an mRNA reference calibration from a dilution series of synthetically generated *bcd* mRNA molecules undergoing the same procedure in parallel (Supplemental Experimental Procedures and Figure S2). To measure the number of *bcd* mRNAs by qRT-PCR, the mRNA reference calibration was compared to an embryo series with n = (1, 2, 4, 8) individuals. The comparison in Figure 1C shows two lines, the slope of which is determined by the PCR efficiency (ε), whereas their offsets (Δ) depend on the combined efficiency of mRNA isolation and reverse transcription (η). These quantities were measured with independent calibrations, which minimize our experimental error (Supplemental Experimental Procedures). Specifically, we first used a dilution series of *bcd* DNA molecules to precisely measure the slope (S = −1/log(ε)), with an accuracy of better than 1%. We used this slope in order to perform one-parameter fits for the mRNA calibration and

embryo series and thus determine the offset (Δ). The number of mRNAs per embryo is then given by $M_{bcd}^{PCR} = M_{\text{ref}}\varepsilon^{-\Delta}$, where M_{ref} is the number of synthetic mRNAs of the lowest member of the mRNA dilution series.

Using this technique, we found the number of *bcd* mRNA molecules in embryos from wild-type females to be $M_{bcd}^{PCR} = (7.4 \pm 1.1) \times 10^5$, where the error represents the measurement error on the mean number of mRNAs per embryo. *stau⁻* embryos contain a similar number of *bcd* mRNA molecules ($M_{bcd,stau⁻}^{PCR} = (6.2 \pm 1.9) \times 10^5$; Figure 1D). These results confirm that, within measurement error, (1) single-molecule FISH counts indeed correspond to individual mRNAs, and (2) *bcd* mRNA counts in *stau⁻* mutant embryos are equivalent to counts in wild-type embryos.

These experiments produced three independent measures for the total *bcd* mRNA count in individual embryos: bulk qPCR measurements on wild-type and *stau⁻* embryos and FISH measurements on *stau⁻* embryos (Figure 1D). To assign a value for our overall estimate, we averaged the three independent measurements, yielding $M_{bcd} = (7.5 \pm 0.8) \times 10^5$ (SEM). The consistency among the three measures validates the FISH-based counting method in assessing embryo-to-embryo *bcd* mRNA count reproducibility.
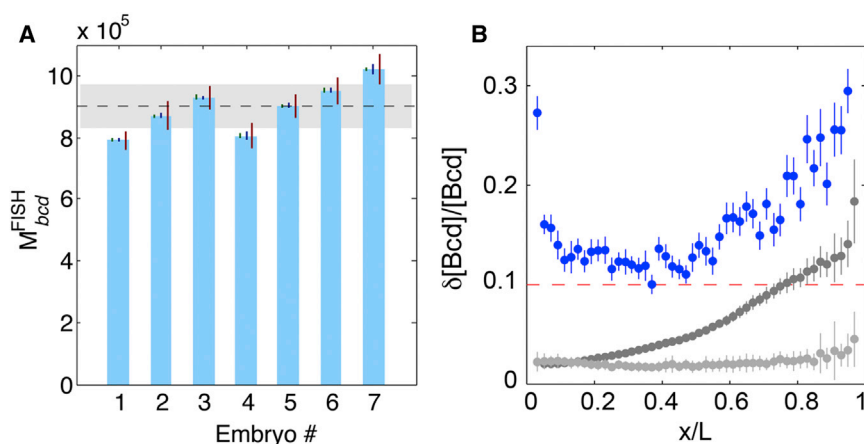
Figure 2. The *bcd* mRNA Source and the Bcd Protein Gradient Are ~10% Reproducible

(A) Total counts of *bcd* mRNA using FISH after density correction in seven individual *stau⁻* embryos. Mean (dashed black line) and SD (gray area) are $(8.9 \pm 0.8) \times 10^5$, which leads to a reproducibility of $0.8/8.9 \sim 9\%$.

(B) Reproducibility of Bcd protein profiles of 22 embryos expressing Bcd-GFP at wild-type Bcd levels (reference fly line Bcd2X$_A$ [14]). Average nuclear Bcd-GFP intensities from the midsagittal plane of all embryos (imaged live during nuclear cycle 14; on average 85 nuclei per embryo) are binned in 50 bins, over which the mean and SD were computed. For each bin, the SD divided by the mean ($\delta[Bcd]/[Bcd]$) as a function of fractional egg length (x/L) is shown in blue (error bars are computed by bootstrapping with 15 embryos [7]). Gray and black lines show estimated contributions of measurement noise (see Supplemental Experimental Procedures). Dashed red line indicates 10% reproducibility mark, attained when subtracting gray from blue data.

Maternally Deposited mRNA Molecules Are as Reproducible as Zygotic Patterns

FISH allows counting of single molecules with measurement error low enough to assess embryo-to-embryo variability, which is impossible to assess with the PCR bulk measurements due to the large systematic error. We estimate our overall measurement error for FISH to be 6% of the total counts (Figure 2A and Supplemental Experimental Procedures). We measured the embryo-to-embryo reproducibility as the SD of *bcd* mRNA counts in seven *stau⁻* mutant embryos (Figure 2A). Strikingly, the result was 9% ± 2% (bootstrapping error). As can be seen in Figure 2B, this level of reproducibility is of the same order as that of the Bcd protein gradient in the anterior half of the embryo (~10% [7]). The similarity suggests that the low variability in *bcd* mRNA production is responsible for the reproducibility of the protein gradient. This is consistent with the idea that the large number of mRNA molecules minimizes the variability inherent to the processes of translation and protein transport, thus obviating requirements for error correction by a separate process.

mRNA and Protein Counts Scale Linearly with Maternal Gene Dosage

The consistency of the reproducibility levels in Figure 2 indicates that control over the mRNA source composition is sufficiently precise to generate a reproducible Bcd gradient. The question remains, however, how such reproducibility is achieved at the mRNA level, and, in particular, whether error correction and feedback mechanisms are required to ensure the correct degree of *bcd* gene expression during oogenesis. In *Drosophila*, 15 specialized germline cells, called nurse cells, remain associated with the oocyte by intercellular cytoplasmic bridges. Nurse cells synthesize maternal components necessary for early embryonic development at high rates and transport them to the growing oocyte over a >2.5-day period, enabling oogenesis to proceed rapidly (reviewed in [24]). High levels of gene expression are facilitated by extensive DNA replication. Such polyploidization generates multiple gene copies in nurse cells, though not necessarily covering the entire genome [25], rendering polyploidization a potentially error-prone process [26]. Thus, it is unclear what mechanisms generate the observed 10% reproducibility levels, or whether error correction is necessary.

To understand the mechanisms controlling the transitions from one molecular species to the next, we examined the link between the maternal *bcd* gene dosage and both *bcd* mRNA and Bcd protein numbers in the embryo. First, using qRT-PCR, we assessed how the number of deposited *bcd* mRNA molecules scales with *bcd* gene copy number. We compared our measurements in wild-type to a strain in which one copy of the *bcd* gene was deleted. The number of *bcd* mRNA molecules in embryos from these *bcd*-deficient (+/Df *bcd*) flies was 0.57 ± 0.14 times that of wild-type embryos with two *bcd* alleles (Figure 1E). The measurement is well within the measurement error of the expected factor of 2, consistent with previously observed differences in relative mRNA levels [27].

Although these measurements are consistent with a linear relationship between *bcd* dosage and actual *bcd* mRNA numbers in the embryo, to achieve a more precise measurement with more than two data points, we took advantage of a strategy exploiting the chromosome position effect [28] to generate small changes in the levels of maternal *bcd* gene product. Transgene constructs expressing Bcd-GFP fusion proteins are inserted at random locations in the fly genome, leading to distinct expression rates and quantitatively different spatial Bcd-GFP distributions [14]; i.e., the same integer copy number generates distinct transcript numbers compared to a calibrated transgenic reference fly line producing Bcd-GFP at wild-type levels (Figure 3, top inset; Figure S3). Using this strategy, we generated a set of six transgenic fly lines, with changes in gene expression levels at increments of 10%. Genetic combinations of individual *bcd-gfp* alleles yield expression levels in the resulting lines that are, within error bars, the sum of the expression levels of the original lines (gray data points in Figure 3), as observed in [14].

To test whether this linear relationship is also preserved at the level of *bcd* mRNA, we repeated our qPCR experiments to measure relative mRNA levels between wild-type and three fly lines expressing Bcd-GFP at 1.78-, 2.12-, or 2.4-fold-increased levels from a total of four or six transgenes (Figure S4). For the same fly lines, we measured the total amount of Bcd-GFP by optically calibrating GFP intensity to that of a purified GFP solution of known molarity [7]. As Figure 3 shows, a scatterplot of Bcd-GFP protein versus mRNA number demonstrates a linear relationship, perfectly matching previous
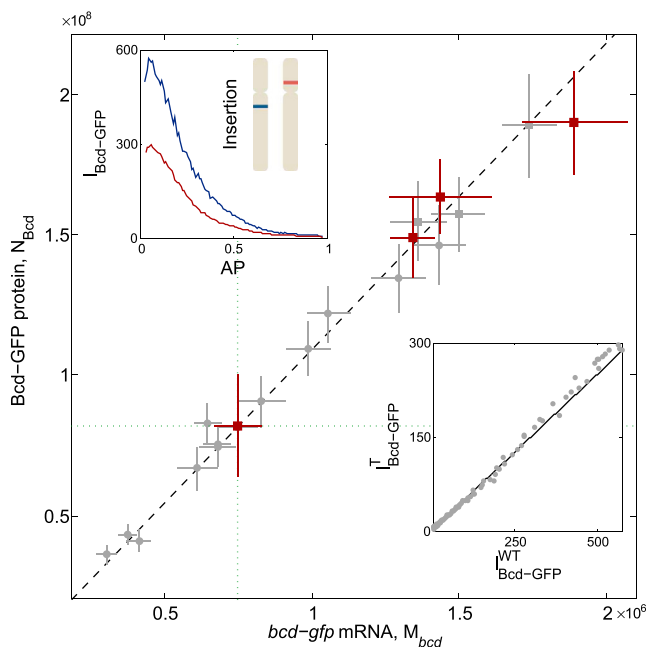
Figure 3. Total Bcd Protein in Embryos Scales Linearly with Maternal *bcd* Gene Expression

Bcd-GFP transgenes are inserted at different genome locations to generate alleles with varying *bcd* gene expression [14]. Insertions in two such fly lines (red and blue bands in top inset) are expressed at different rates, leading to quantitatively different Bcd protein intensity profiles $I_{Bcd-GFP}$ (Figure S3). Differences in protein concentration are determined by comparing average nuclear Bcd-GFP intensities across AP positions between a given transgenic test line (I^T) and a reference line (I^{WT}). The latter expresses *egfp-bcd* mRNA at the same level as endogenous *bcd* mRNA (Figure S4B) and produces Bcd-GFP at wild-type levels that restore normal patterning to *bcd* mutants. The slope of a line fitted to a scatterplot of intensities defines the Bcd-GFP expression level of the test line relative to the reference line (bottom inset; in this example, 21 and 108 embryos of the test and reference lines, respectively). The main panel shows a scatterplot of Bcd-GFP protein expression versus *bcd-gfp* mRNA expression measured by PCR (Figure S4A) in embryos from four fly lines (red squares). The relationship between protein expression and number of deposited mRNAs in the embryo is linear. For 18 fly lines, the gray data points correspond to Bcd-GFP expression of genetically combined alleles (wild-type calibrated to GFP standard) as a function of the sum of the separately measured *bcd-gfp* mRNA expression levels of the individual alleles (calibrated to wild-type mRNA counts). Wild-type is marked by vertical and horizontal dotted green lines. To calculate *bcd-gfp* mRNA expression, we measured Bcd-GFP protein expression [14] for each allele and converted it to mRNA expression (Figure S4A). Squares identify respective fly lines in four of the gray data sets and in the four red data sets. The linear relationship demonstrates that expression levels of individual alleles add independently in a linear feedforward manner. Gray error bars are as quantified previously [14]. Red error bars are SDs in expression level measurements; red error bars of data point of reference fly line (Bcd2X_A; crossing of dotted lines) represent calibration error to total molecular counts for protein and mRNA, respectively (Supplemental Experimental Procedures).

data from protein measurements [14]. Together, our observations indicate a scenario in which the transition from one molecular species to another is achieved in a perfectly linear feedforward manner. Specifically, small changes in the strength of the maternal *bcd* gene lead to proportional changes in both mRNA and protein counts in the embryo. All molecular processes from maternal gene expression to protein synthesis in the embryo must operate with very high precision, for which the protein measurements give an estimate:

10% changes in *bcd* strength at the level of maternal DNA are reflected as 10% changes in protein copy numbers.

Finally, measurements of both mRNA and protein numbers provide unique quantitative access to *bcd* translation. Bcd-GFP protein levels are linearly proportional to *bcd* and *gfp* mRNA amounts (Figure S4A), and the transgenic reference line produces the same amount of mRNA as the endogenous *bcd* locus, as determined by measuring *bcd* and *gfp* mRNA levels in the same embryos (Figure S4B). Previous intensity measurements of fluorescently tagged *bcd* mRNAs have shown that they are not degraded and remain stable throughout the first 2 hr of development (i.e., early nuclear cycle 14) [20]. During this period, Bcd protein is degraded uniformly with a lifetime of $\tau = 50$ min [29]. In the simplest model, Bcd translation is uniform, and the number of expressed proteins at time *t* is given by $N_{Bcd}(t) = k\tau M_{bcd}(1 - \exp(-t/\tau))$, where k is the translation rate and M_{bcd} is the number of *bcd* mRNAs. Using GFP calibration [7], we measured the total amount of Bcd-GFP in fixed embryos in which all Bcd-GFP proteins mature and become optically detectable [18]. We found a total of $N_{Bcd} = (8.2 \pm 1.8) \times 10^7$ (SD) Bcd-GFP molecules in approximately 2-hr-old embryos (i.e., $t_{14} = 146$ min). The value is larger than earlier estimates in live embryos [7] due to the maturation correction [18] and lower than semiquantitative biochemical measurements [29] (see Supplemental Experimental Procedures). Thus, with $M_{bcd} = (7.5 \pm 0.8) \times 10^5$ mRNA molecules, we calculated a translation rate of $k \approx 2$ proteins per mRNA per minute, which matches previously reported translation rates during the development of sea urchin embryos [30].

Discussion

We developed protocols to count the number of *bcd* mRNA molecules in individual *Drosophila* embryos. The total number is quite large, approaching one million molecules, and it is reproducible between embryos, with fluctuations of less than 10%. Such low-level fluctuations were previously observed for the Bcd protein gradient. Our present results support the idea that reproducibility is determined during oogenesis by females expressing a tightly controlled number of *bcd* mRNAs. These data show that the processes that establish the protein gradient, from maternal *bcd* DNA to Bcd protein in the zygote, are governed by linear feedforward mechanisms, which minimize requirements for error correction during gradient formation.

Our results are consistent with work showing that the segmentation gene network of early embryos acts as a relay to propagate molecular reproducibility [7, 11, 12, 14, 20, 31]. After 3 hr, cellular identities are generated with single-cell precision, as observed in gene expression patterns that arise downstream of maternal inputs and that result in morphogenetic events (e.g., the formation of the cephalic furrow). Here, we have added another element upstream of that cascade, demonstrating that reproducibility in the embryo is established during oogenesis through precise control over *bcd* mRNA expression. Hence, morphological features emerge reproducibly between embryos as a result of the precision with which the female controls initial patterning signals. The early segmentation cascade in the *Drosophila* embryo is therefore a striking example of a molecular network integrating precise initial conditions to achieve reproducible macroscopic outcomes. Thus, at least for wild-type embryos in the laboratory, early patterning does not require independent system(s) to monitor or correct fluctuations in molecular activities during

the transitions between mRNA and protein or between maternal inputs and zygotic outputs.

Given high levels of reproducibility, our finding that molecular signals are transmitted in a linear feedforward manner seems surprising. Feedforward processes have a propensity for escalating noise, yet we found that changes as low as 10% in *bcd* mRNA result in 10% changes in protein. Thus, the network establishing the Bcd gradient maintains precision at each transition between different molecular species. Particularly, reproducible *bcd* mRNA counts and the proportionality to maternal copy number indicate that the synthesis and transport of mRNA are precisely controlled and proceed essentially identically in different females. Here, control over molecular fluctuations is achieved by temporal and spatial averaging and by large molecule numbers. Nearly one million *bcd* mRNA molecules are generated, completely overriding Poisson fluctuations, matching other systems in which high mRNA levels reduce variability [32, 33]. Moreover, *bcd* is generated from multiple (>500) *bcd* DNA sources in polyploid nurse cells [34, 35] over a period of several days [24, 36]. This is conducive to spatial and temporal averaging, particularly when comparing this time course to the timescale of microscopic events, such as the synthesis of a single mRNA molecule.

Finally, the linear response in Bcd amounts to changes in the maternal gene copies indicates identical *bcd* translation kinetics across embryos and hence tight control over translation rates [37]. After fertilization, mRNA translation and establishment of the Bcd gradient require only ~1 hr. Thus, we expect that the translational apparatus operates at near maximal rate in the early embryo. However, the translation of *bcd* mRNA is an order of magnitude lower than the typical translation rate for eukaryotic organisms under optimal conditions [38, 39] (Supplemental Experimental Procedures). We suggest that to achieve reproducibility, embryos employ a lower-than-maximal translation rate with large numbers of source mRNA molecules, facilitating spatial and temporal averaging [7, 20, 40]. How these interactions are matched to produce reliable patterning remains unknown. Overall, the Bcd gradient as a paradigm for morphogen-mediated patterning now presents an ideal system to analyze how molecular networks are coordinated to maintain precision and reproducibility.

Experimental Procedures

FISH, confocal microscopy, and image analysis were performed as described in [18, 20], where capability of capturing all mRNA molecules in whole embryos was demonstrated. qRT-PCR quantification of transcripts in embryos was carried out with SYBR Green on an Applied Biosystems 7900HT Fast Real-Time PCR system using standard temperature protocol and automatic threshold detection. The absolute amount of *bcd* mRNA in extracts and of Bcd-GFP in live embryos is measured by calibration fluorescence standards (see Supplemental Experimental Procedures). All animal usage is under the approval of Princeton University's Institutional Animal Care and Use Committee.

Supplemental Information

Supplemental Information includes Supplemental Experimental Procedures, four figures, and two tables and can be found with this article online at http://dx.doi.org/10.1016/j.cub.2014.04.028.

Acknowledgments

References

1. Thompson, D.W. (1942). On Growth and Form (Cambridge: Cambridge University Press).
2. Maynard-Smith, J. (1960). Continuous, quantized and modal variation. Proc. R. Soc. Lond. B. *152*, 397–409.
3. Lawrence, P.A. (1973). In Developmental Systems: Insects, *Volume 2*, Doane, W.W., Counce, S.J., and Waddington, C.H., eds. (New York: Academic Press), p. 157.
4. Kerszberg, M., and Wolpert, L. (2007). Specifying positional information in the embryo: looking beyond morphogens. Cell *130*, 205–209.
5. Arias, A.M., and Hayward, P. (2006). Filtering transcriptional noise during development: concepts and mechanisms. Nat. Rev. Genet. *7*, 34–44.
6. Driever, W., and Nüsslein-Volhard, C. (1988). A gradient of bicoid protein in Drosophila embryos. Cell *54*, 83–93.
7. Gregor, T., Tank, D.W., Wieschaus, E.F., and Bialek, W. (2007). Probing the limits to positional information. Cell *130*, 153–164.
8. Jaeger, J. (2011). The gap gene network. Cell. Mol. Life Sci. *68*, 243–274.
9. Gergen, J.P., Coulter, D., and Wieschaus, E.F. (1986). Segmental pattern and blastoderm cell identities. In Gametogenesis and the Early Embryo, J.G. Gall, ed. (New York: Alan R. Liss, Inc.), pp. 195–220.
10. Crauk, O., and Dostatni, N. (2005). Bicoid determines sharp and precise target gene expression in the Drosophila embryo. Curr. Biol. *15*, 1888–1898.
11. Dubuis, J.O., Samanta, R., and Gregor, T. (2013). Accurate measurements of dynamics and reproducibility in small genetic networks. Mol. Syst. Biol. *9*, 639.
12. Houchmandzadeh, B., Wieschaus, E., and Leibler, S. (2002). Establishment of developmental precision and proportions in the early Drosophila embryo. Nature *415*, 798–802.
13. Surkova, S., Kosman, D., Kozlov, K., Manu, Myasnikova, E., Samsonova, A.A., Spirov, A., Vanario-Alonso, C.E., Samsonova, M., and Reinitz, J. (2008). Characterization of the Drosophila segment determination morphome. Dev. Biol. *313*, 844–862.
14. Liu, F., Morrison, A.H., and Gregor, T. (2013). Dynamic interpretation of maternal inputs by the Drosophila segmentation gene network. Proc. Natl. Acad. Sci. USA *110*, 6724–6729.
15. Namba, R., Pazdera, T.M., Cerrone, R.L., and Minden, J.S. (1997). Drosophila embryonic pattern repair: how embryos respond to bicoid dosage alteration. Development *124*, 1393–1403.
16. Vincent, A., Blankenship, J.T., and Wieschaus, E. (1997). Integration of the head and trunk segmentation systems controls cephalic furrow formation in Drosophila. Development *124*, 3747–3754.
17. Gierer, A. (1991). Regulation and reproducibility of morphogenesis. Semin. Dev. Biol. *2*, 83–93.
18. Little, S.C., Tkačik, G., Kneeland, T.B., Wieschaus, E.F., and Gregor, T. (2011). The formation of the Bicoid morphogen gradient requires protein movement from anteriorly localized mRNA. PLoS Biol. *9*, e1000596.
19. Ferrandon, D., Elphick, L., Nüsslein-Volhard, C., and St Johnston, D. (1994). Staufen protein associates with the 3'UTR of bicoid mRNA to form particles that move in a microtubule-dependent manner. Cell *79*, 1221–1232.
20. Little, S.C., Tikhonov, M., and Gregor, T. (2013). Precise developmental gene expression arises from globally stochastic transcriptional activity. Cell *154*, 789–800.
21. Bustin, S.A. (2004). A–Z of Quantitative PCR (La Jolla: International University Line).
22. Bustin, S.A., Benes, V., Garson, J.A., Hellemans, J., Huggett, J., Kubista, M., Mueller, R., Nolan, T., Pfaffl, M.W., Shipley, G.L., et al. (2009). The MIQE guidelines: minimum information for publication of quantitative real-time PCR experiments. Clin. Chem. *55*, 611–622.
23. Nolan, T., Hands, R.E., and Bustin, S.A. (2006). Quantification of mRNA using real-time RT-PCR. Nat. Protoc. *1*, 1559–1582.

24. Spradling, A. (1993). Developmental genetics of oogenesis. In The Development of *Drosophila melanogaster*, *Volume 1*, Bate, M., and Arias, A.M., eds. (Cold Spring Harbor: Cold Spring Harbor Laboratory Press), pp. 1–70.

25. Claycomb, J.M., and Orr-Weaver, T.L. (2005). Developmental gene amplification: insights into DNA replication and gene expression. Trends Genet. *21*, 149–162.

26. Fox, D.T., Gall, J.G., and Spradling, A.C. (2010). Error-prone polyploid mitosis during normal Drosophila development. Genes Dev. *24*, 2294–2302.

27. Cheung, D., Miles, C., Kreitman, M., and Ma, J. (2011). Scaling of the Bicoid morphogen gradient by a volume-dependent production rate. Development *138*, 2741–2749.

28. Markstein, M., Pitsouli, C., Villalta, C., Celniker, S.E., and Perrimon, N. (2008). Exploiting position effects and the gypsy retrovirus insulator to engineer precisely expressed transgenes. Nat. Genet. *40*, 476–483.

29. Drocco, J.A., Grimm, O., Tank, D.W., and Wieschaus, E. (2011). Measurement and perturbation of morphogen lifetime: effects on gradient shape. Biophys. J. *101*, 1807–1815.

30. Bolouri, H., and Davidson, E.H. (2003). Transcriptional regulatory cascades in development: initial rates, not steady state, determine network kinetics. Proc. Natl. Acad. Sci. USA *100*, 9371–9376.

31. Dubuis, J.O., Tkacik, G., Wieschaus, E.F., Gregor, T., and Bialek, W. (2013). Positional information, in bits. Proc. Natl. Acad. Sci. USA *110*, 16301–16308.

32. Thattai, M., and van Oudenaarden, A. (2001). Intrinsic noise in gene regulatory networks. Proc. Natl. Acad. Sci. USA *98*, 8614–8619.

33. Ozbudak, E.M., Thattai, M., Kurtser, I., Grossman, A.D., and van Oudenaarden, A. (2002). Regulation of noise in the expression of a single gene. Nat. Genet. *31*, 69–73.

34. Dej, K.J., and Spradling, A.C. (1999). The endocycle controls nurse cell polytene chromosome structure during Drosophila oogenesis. Development *126*, 293–303.

35. King, R.C. (1970). Ovarian Development in *Drosophila melanogaster* (New York: Academic Press).

36. Becalska, A.N., and Gavis, E.R. (2009). Lighting up mRNA localization in Drosophila oogenesis. Development *136*, 2493–2503.

37. Bialek, W. (2012). Biophysics: Searching for Principles (Princeton: Princeton University Press).

38. Bonven, B., and Gulløv, K. (1979). Peptide chain elongation rate and ribosomal activity in Saccharomyces cerevisiae as a function of the growth rate. Mol. Gen. Genet. *170*, 225–230.

39. Qin, X., Ahn, S., Speed, T.P., and Rubin, G.M. (2007). Global analyses of mRNA translational control during early Drosophila embryogenesis. Genome Biol. *8*, R63.

40. Erdmann, T., Howard, M., and ten Wolde, P.R. (2009). Role of spatial averaging in the precision of gene expression patterns. Phys. Rev. Lett. *103*, 258101.